Electronic Supplementary Material (ESI) for Chemical Science.

A Noble Metal-Free Proton-Exchange Membrane Fuel Cell based on Bio-inspired Molecular Catalysts

P. D. Tran,[a#] A. Morozan,[b#] S. Archambault,[c#] J. Heidkamp,[d#] P. Chenevier,[e] H. Dau,[d] M. Fontecave,[af] A. Martinent,[c*] B. Jousselme,[b*] V. Artero[a*]

[a] *Laboratoire de Chimie et Biologie des Métaux ; Université Grenoble Alpes, CNRS, CEA; 17 rue des Martyrs, 38054 Grenoble cedex 09, France*

[b] *CEA Saclay, IRAMIS, NIMBE, Laboratory of Innovation in Surface Chemistry and Nanosciences (LICSEN), Gif sur Yvette, France.*

[c] *Institut LITEN CEA LITEN/DTNM/LCSN, Grenoble, France*

[d] *FB Physik, Free University Berlin, Berlin, Germany*

[e] *Université Grenoble Alpes, CNRS, CEA, INAC-SPRAM, F-38000 Grenoble, France*

[f] *Collège de* France, 11 place Marcelin Berthelot 75005 Paris, France.

[#] *these authors equally contributed to the work*

Materials

$[Ni(P^{Ph}{}_2N^{CH2Pyrene}{}_2)_2](BF_4)_2$ was prepared as previously described.[1] Cobalt(II) nitrate hexahydrate ($Co(NO_3)_2 \cdot 6H_2O$), 1H-1,2,3-triazolo[4,5-b]pyridine (TAPy) and Nafion 117 solution (5 wt. % in a mixture of alcohols and water) were purchased from Sigma Aldrich. Vulcan XC-72 was supplied from FuelCellStore. Commercial grade C100 Multi-walled Carbon Nanotubes (MWCNTs, > 95 %) were obtained from Nanocyl and used as received, without any purification. The electrolyte used, 0.5 M H_2SO_4 aqueous solution, was prepared with ultrapure water (18.2 MΩ·cm). All gases (nitrogen, oxygen) were 99.995 % purity.

Synthesis

Cobalt/nitrogen/Vulcan (Co-N-C) cathode catalyst (12 wt. % is the nominal weight percentage of Co over the TAPy-CNTs mixture, 2/1 is the mass ratio of TAPy to CNTs) was prepared as follows. 1H-1,2,3-triazolo[4,5-b]pyridine (TAPy) (400 mg) was added to a solution of $Co(NO_3)_2 \cdot 6H_2O$

(355.1 mg) in ethanol (30 mL) and the solution was stirred for 2 h at 60 ºC. Then, a dispersion of Vulcan XC-72 (200 mg) in ethanol (100 mL) was ultrasonicated for 30 min and added to the previous solution. The mixture was heated under reflux at 60 ºC for 5 h. Ethanol was removed under reduced pressure to give a black Co–TAPy-Vulcan powder which was subsequently placed for 2 h in a tube furnace under a flux of Ar to remove residual air, heated at 5 ºC·min^{-1} until 700 °C, held at this temperature for 1 h and then cooled at 5 ºC·min^{-1} until room temperature, the whole procedure being achieved in a flowing Ar atmosphere. Detailled characterization of Co-N-C and its ORR performances are provided below.

Anode catalyst was prepared by suspending [Ni($P^{Ph}_2N^{CH2Pyrene}_2$)$_2$](BF$_4$) (40 mg) and MWCNTs (30 mg) in CH_3CN (100 mL). After 10 min sonication, Vulcan XC-72 (30 mg) was added to the solution and the suspension was sonicated for 5 more min. The solvent was then evaporated in vacuo.

Inks were prepared by mixing anode or cathode catalyst with 5wt. % Nafion® solution in hydro-alcoholic solution. The mixtures were sonicated for 1 h. Isopropanol was added to the catalyst ink which was sonicated again for 30 min. The Nafion® polymer and the catalyst are respectively 20-30 wt. % and 70-80 wt. % of the total solid content of the catalyst inks. The particle size distribution in inks was determined by laser granulometry. A typical granulogram of the anode catalyst is shown on Figure S1.

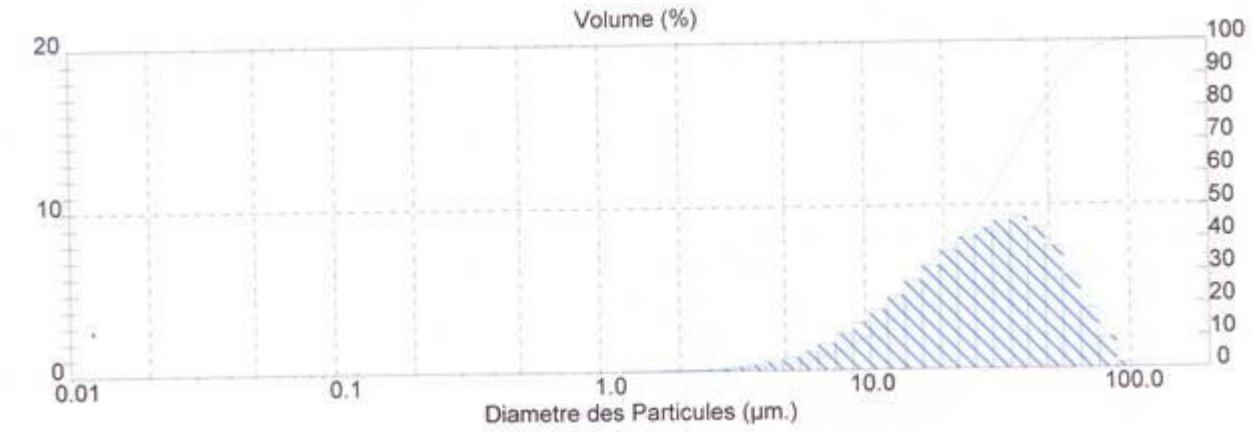

Figure S1. Granulometry particle size histogram for the anode catalyst.

Membrane electrode assembly (MEA) fabrication

The catalyst suspensions are directly sprayed using an air brush (Harder and Stenbeck) to both sides on NRE-212 Nafion® perfluorosulfonic acid membranes commercialised by DuPont™. The membrane is used without pretreatment steps and attached on glass with adhesive tape. The deposition is carried out at 60-80 °C on a hot plate in order to evaporate both the water in the membrane and the solvent in the catalyst ink. Both sides are subsequently sprayed and the resultant MEA is dried for one night in the air at room temperature.

The MEA is then pressed at 50 °C under a pressure of 0.2 MPa for 3 min. The active electrode area was 5.76 cm². Gold was deposited by physical vapor deposition, thin enough to let H_2 and O_2 reach catalysts sites but thick enough to ensure a good collect of current.

MEA electrochemical characterization

MEAs electrochemical characterization were performed at 60 °C in a fuel cell test chamber. A scheme of the chamber is given on Figure S2. Air is supplied to the cathode by natural convection at atmospheric pressure. Hydrogen (flow rate: 20 $mL \cdot min^{-1}$) was humidified by passing through bubbling in water before supply to the fuel cell anode chamber.

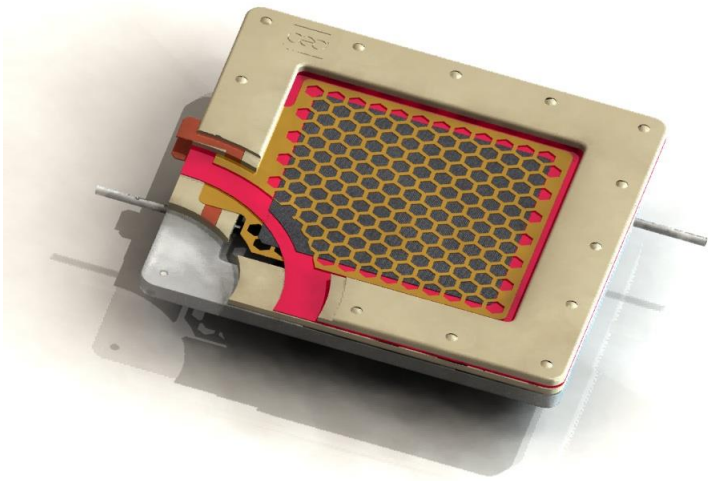

Figure S2. Artistic view of the fuel cell test chamber. The Nafion membrane is depicted in red. The catalytic cathode (top) and anode (bottom) catalytic layers are depicted in dark grey. The gold honey combs are the current collectors made of gold. The metal support below is the hydrogen chamber fed through by the inlet and outlet metallic tubes. The anode is in contact with air through the gold collector.

Electrochemical tests were performed with a Bio-Logic system VMP model in a climatic chamber. After measuring open circuit voltages (OCV), polarization measurements were performed at stationary conditions, after equilibration of current density for 8 min at each applied potential. Cyclic voltammetry (CV) curves were achieved between 0.2 V and the OCV at 2 $mV \cdot s^{-1}$ scan rate. The impedance measurements were carried out at a cell voltage of 0.4 V, with an AC frequency range of 100 kHz to 100 mHz and a sinusoidal amplitude of 10 mV.

X-ray absorption spectroscopy (XAS) studies

XAS measurements at the cobalt and nickel *K*-edge were performed at beamline KMC-1 of the Helmholtz-Zentrum Berlin for Materials and Energy (formerly BESSY II).[2] Spectra were collected at 20 K in absorption and fluorescence mode as described elsewhere.[3] The scan range of the excitation energy was 7580-8750 eV for Co and 8150-9390 eV for Ni. The energy windows of the single channel analysers for the 13 elements of the fluorescence detector were accordingly set to the K_α-emission of Co or Ni. If necessary, a 10 µm thick filter foil of Fe or Co was put between sample and detector to suppress scattered light when measuring Co or Ni emission, respectively. For energy calibration, the energy axis of the experimental data was shifted by an offset such that the first maximum in the derivative of the reference absorption of a Co or a Ni foil (5 µm thick) aligned with the corresponding value of 7709 eV or 8333 eV for the 1st inflection point of the Co or Ni *K*-edge, respectively (values reported by Bearden and Burr).[4] The extended x-ray absorption fine-structure (EXAFS) oscillations at the Co *K* edge were extracted by minimizing a "knot-spline" with 7 knots between 7730 - 8310 eV or 8350-8930 eV for the Co or Ni *K*-edge (corresponding data *k*-range ≈ 2 - 13 $Å^{-1}$), respectively, which then was subtracted from the data. The extracted EXAFS were weighted with k^3 to amplify oscillations in the higher *k*-range. Then, the EXAFS was Fourier-transformed. To suppress side-lobe artefacts of the transformation, a cosine window function was applied covering the first and last 10% of the data *k*-range in the case of the Co spectra and the first 10% and last 50% of the data range in the case of the Ni spectra.

Microcrystalline $[Ni(P^{Ph}{}_2N^{CH2Pyrene}{}_2)_2](BF_4)_2$, as-prepared Ni-CNT material, as-prepared microcrystalline Co-N-C material, $LiCo^{III}O_2$ and $[Co^{II}(OH_2)_6](NO_3)_2$ were thoroughly mixed with boron nitride to obtain homogeneous samples of appropriate optical thickness. $Ni(OH_2)_6]^{2+}$ was prepared by solving $NiCl_2$ in deionized water (10 mM) and freezing the solution in liquid nitrogen.

The anode catalyst was deposited onto gas-diffusion layers (same preparation as previously described but without application of the Nafion® membrane[1]). These electrodes were characterized as prepared and after electrochemical equilibration in 0.5 M H_2SO_4 aqueous solution (by repeating 5 potential cycles (potential scan rate of 2 $mV \cdot s^{-1}$) from –0.3 V to +0.5 V *vs.* RHE, Figure S6) or extended turnover for H_2 oxidation (at +0.25 V *vs.* RHE, Figure S7) or evolution (at –0.3 V *vs.* RHE, Figure S8). Then the sample was taken out from the gas-diffusion layer and mixed with boron nitride as described above for measurement.

Detailled characterization of the Co-N-C material and its catalytic performances for oxygen reduction.

XPS characterization

X-ray photoemission spectroscopy (XPS) analyses were performed with a Kratos Axis Ultra DLD using a high-resolution monochromatic Al-Kα line X-ray source at 1486.6 eV. Fixed analyzer pass energy of 20 eV was used for core level scans. Survey spectra were captured at pass energy of 160 eV. The photoelectron take-off angle was always normal to the surface, which provided an integrated sampling depth of approximately 15 nm. All spectra were referenced with an external gold substrate with a binding energy of 84.0 eV for Au 4f.

Electrode preparation for RDE and RRDE studies

The catalyst ink was prepared by dispersing the Co-N-C catalyst (10 mg) in a mixture of ethanol (370 μL), H_2O (150 μL) and Nafion 117 solution (80 μL) under sonication (1h).

The glassy carbon (GC) disk substrate for RDE and RRDE studies (∅ 5 mm, 0.1963 $cm^2_{geom.}$) was polished with aqueous dispersions of synthetic diamond (1 μm), rinsed and sonicated in water before each measurement.

The catalyst layer was obtained by dropping 5 μL of the ink onto the GC disk and the disk was dried under air environment. The final catalyst loading is 425 $\mu g \cdot cm^{-2}$.

Electrochemical characterization

A typical three-electrode glass cell was used. Experiments were controlled using a VSP bipotentiostat (Bio-Logic SAS). A speed control unit-Princeton Applied Research Model 636 Electrode Rotator and a Pine rotating ring-disk electrode (RRDE) with GC disk and Pt ring were also used. Saturated KCl calomel electrode (SCE) and a graphite plate were used as reference

electrode and counter electrode respectively. All potentials reported refer to that of SCE.

A 5 $mV \cdot s^{-1}$ scan rate was applied for the RDE studies. Polarization curves were recorded with various rotation rates (ω) of 400, 800, 1200, 1600 and 2000 rpm. RDE plots ($1/j_{app}$ *vs.* $1/\omega^{1/2}$), were analyzed according to the Koutecky–Levich (K-L) equation expressed as Eq. 1 to assess the apparent number of electrons transferred during ORR (n) at various potentials:[5]

$$1/j_{app} = 1/j_k + 1/j_{\lim} = 1/nFC_{O_2}k_{O_2}\Gamma + 1/0.62nFC_{O_2}D_{O_2}^{2/3}\nu^{-1/6}\omega^{1/2} \quad (1)$$

where n can be extracted from the slope; j_{app} is the measured or apparent current density ($A \cdot cm^{-2}$); j_k is the kinetic current density ($A \cdot cm^{-2}$); j_{lim} is the limiting current density ($A \cdot cm^{-2}$); F is Faraday's constant ($C \cdot mol^{-1}$); C_{O2} is the concentration of oxygen ($mol \cdot cm^{-3}$); k_{O2} is the kinetic rate constant for the catalyzed ORR ($cm^2 \cdot s^{-1}$); Γ is the total surface coverage of the catalyst ($mol \cdot cm^{-2}$); D_{O2} is the diffusion coefficient of oxygen in aqueous solution ($cm^2 \cdot s^{-1}$); ν is the kinematic viscosity ($cm^2 \cdot s^{-1}$); and ω is the rotation rate of the electrode ($rad \cdot s^{-1}$).[6, 7]

Current densities were normalized in reference to the geometric area of the GC RDE (0.1963 cm^2).

Stability experiment was carried out using chronoamperometry with the electrode rotation rate fixed at 1000 rpm (E=0.2 V *vs.* SCE) in O_2-saturated 0.5 M H_2SO_4.

Results

The chemical composition of the Co-N-C catalyst was assessed by X-ray photoelectron spectroscopy (XPS). The detailed peak analysis of the XPS spectra is given in Figure S3 and Table S1.

The survey spectrum highlight the presence of carbon, oxygen, nitrogen and cobalt (83.90 % C, 4.42 % O, 10 % N, 1.68 % Co) in agreement with our previous work with carbon nanotubes support.[8]

The deconvolution of N1s core level was realized with four peaks: the presence of the pyridinic-N moieties at 398 eV (N1, reported in the literature from 397 to 399 eV)[9] obtained after annealing at 700 °C that can be explained by the cyclization of neighboring C-N groups after TAPy ring opening.[10] The contribution at 401 eV has been assigned to various forms of quaternary-N (N4, protonated pyridine or graphitic-N).[11] The decomposition of the N 1s peaks reveals also the presence of other N species, as pyrrolic-N (N3, 400.2 eV), or nitrogen complexed with metal in Co-N_x centers (N2, 399 eV).[12] Moreover, the presence of nitrile groups (reported at 399.4±0.2 eV)[8, 12-14] is possible in the binding energy range of N2.

In the Co 2p range, the decomposition of XPS spectra gives many peaks in the Co-N-C catalyst: (1) a peak due to cobalt associated with N in Co–N_x around 781.3 eV, which is consistent with the

corresponding peak detected in the N 1s spectrum (N2), (2) peaks at 780.4 eV and 779.2 eV corresponding to a mixture of cobalt oxides,[15] and (3) a peak at *ca.* 778 eV corresponding to metallic Co.

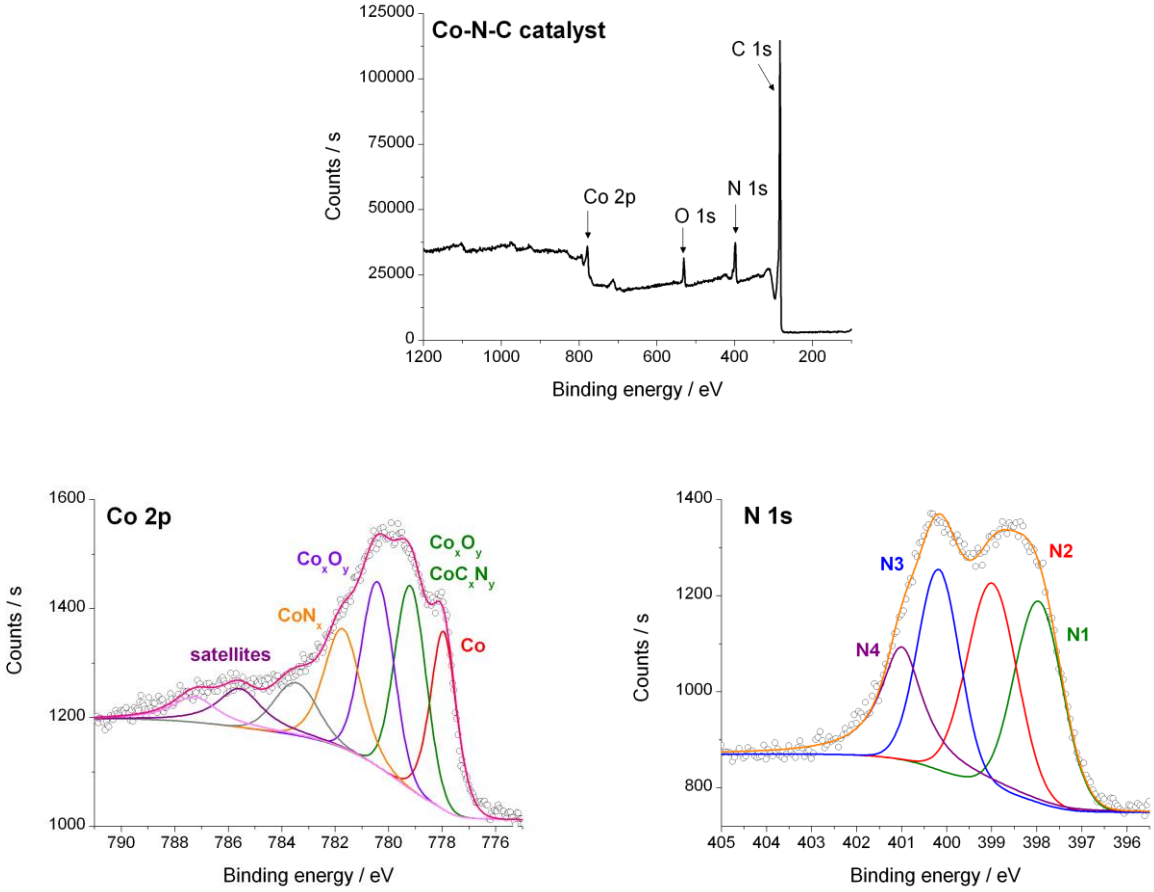

Figure S3. XPS survey spectrum (top) and decomposed N 1s and Co 2p spectra (bottom) of the Co-N-C catalyst.

Table S1. N 1s and Co 2p composition of Co-N-C catalyst from XPS						
N 1s				Co 2p		
Peak number	Component	BE (eV)	Atomic %	Peak component	BE (eV)	Atomic %
N1	N 1s (pyridinic-N)	398.0	27.58	Co	778.0	17.64
N2	N 1s (Co-N_x, nitrile)	399.0	28.96	Co_xO_y, CoC_xN_y	779.2	23.10
N3	N 1s (pyrrolic-N)	400.2	24.16	Co_xO_y	780.4	21.75
N4	N 1s (quaternary-N)	401.0	19.30	Co-N_x	781.3	16.55
				satellites	783.5-787.3	20.96

RDE polarization curves on Co-N-C catalyst at rotation rates from 400 to 2000 rpm (Figure S4) give the apparent number of electrons for O_2 reduction (*n*) from Koutecky–Levich (K-L) plots according to Eq. 1 (n=3.22). Other key parameters specific for the ORR catalytic activity are the onset potential, E_{onset} (480 mV *vs.* SCE), the half-wave potential, $E_{1/2}$ (380 mV *vs.* SCE) and the limiting cathodic current density $j_{l,c}$ (-1.166 mA·cm^{-2} at 1200 rpm).

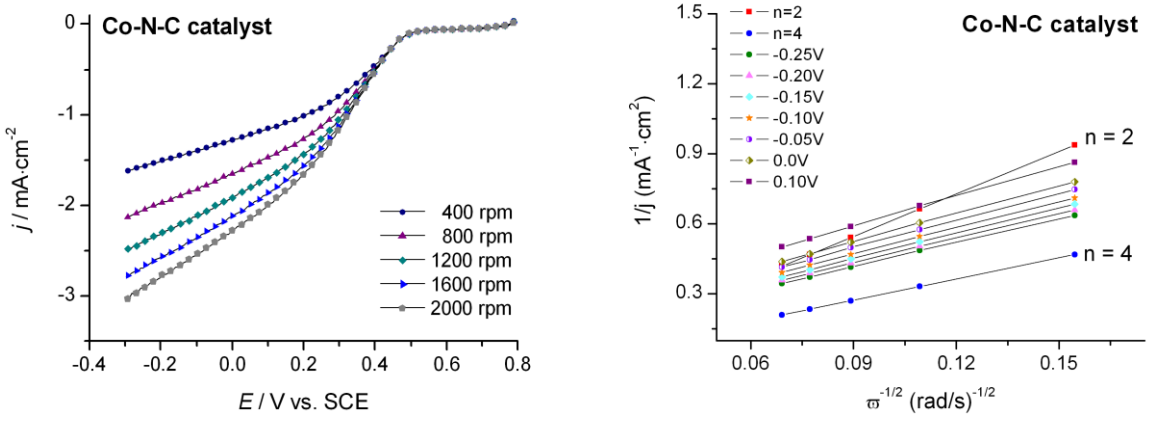

Figure S4. RDE polarization curves at different rotation rates for ORR on Co-N-C catalysts in 0.5 M H_2SO_4, catalyst loading: 425 μg·cm^{-2} and scan rate: 5 mV·s^{-1} (left). Koutecky-Levich plots at different electrode potentials (right).

Stability of ORR catalyst in sulfuric acid solution was assessed by chronoamperometry at 0.2 V vs SCE and 1000 rpm. The curve displayed in Figure S5 show a slight decrease of the performance vs the time of electrolysis. However after 18 h, the catalyts keeps 55 % of the initial electractivity.

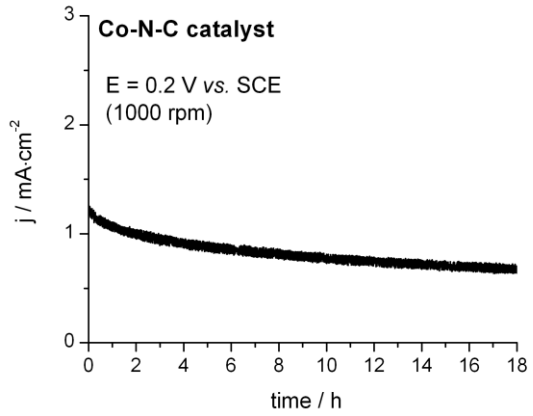

Figure S5. Chronoamperometric curve of the ORR on Co-N-C catalyst in O_2-saturated 0.5 M H_2SO_4 solution at E = 0.2 V *vs.* SCE and 1000 rpm.

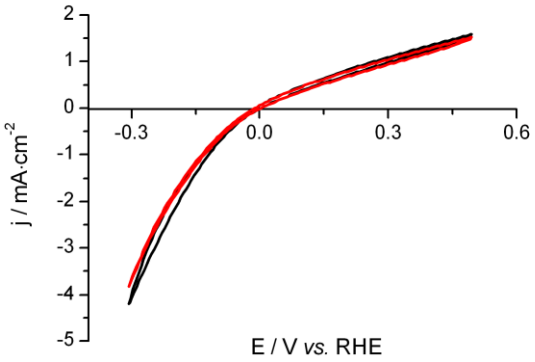

Figure S6: Repeating dynamic potential screenings (potential scan rate of $2mV \cdot s^{-1}$) on a $[Ni(P^{Ph}{}_2N^{CH2Pyrene}{}_2)_2](BF_4)_2$/MWCNTs electrode in pH 0 H_2SO_4 solution. Black curve: 1st scan; Red curve: 5th scan.

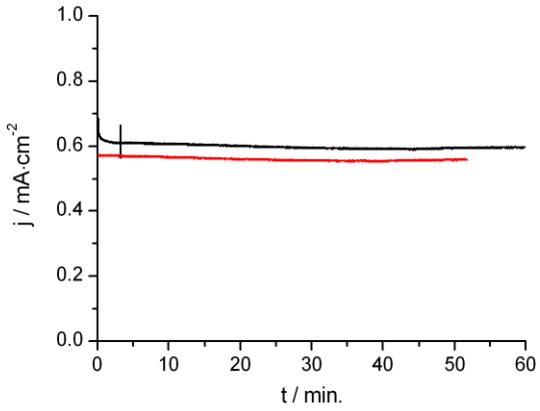

Figure S7: Chronoamperometric curves of $[Ni(P^{Ph}{}_2N^{CH2Pyrene}{}_2)_2](BF_4)_2$/MWCNTs electrodes equilibrated at +0.25 V *vs.* RHE in H_2-saturated pH 0 H_2SO_4 solution. Red curve: electrode coated with Nafion membrane; Black curve: electrode without Nafion coated.

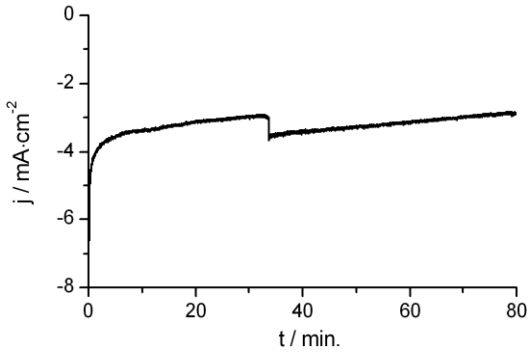

Figure S8: Chronoamperometric curve of a $[Ni(P^{Ph}{}_2N^{CH2Pyrene}{}_2)_2](BF_4)_2$/MWCNTs electrode (without Nafion membrane coated) equilibrated at –0.3 V *vs.* RHE in pH 0 H_2SO_4 solution.

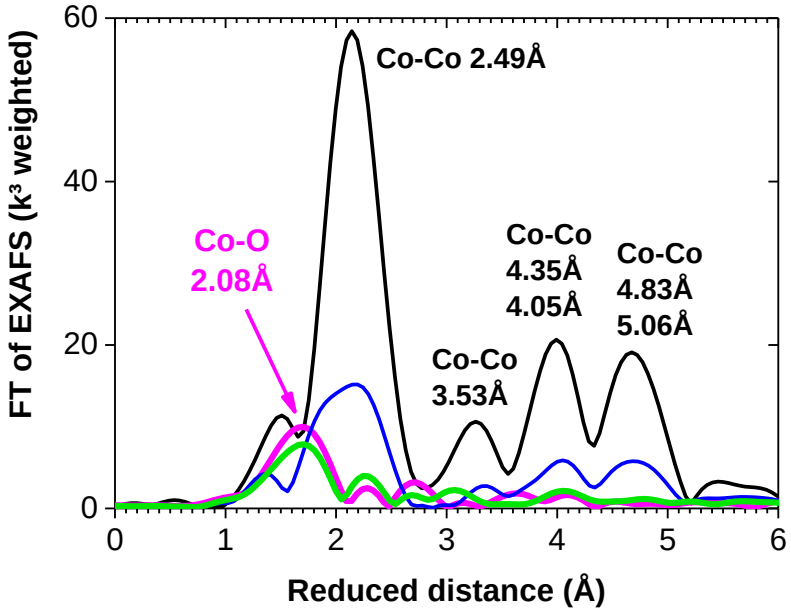

Figure S9: Fourier-transforms (*k*-range from 2 to 13 $Å^{-1}$) of k^3-weighted EXAFS spectra (Co *K*-edge) of Co-N-C material after O_2-reduction catalytic operation (blue line), of purely metallic Co^0 (black line) and of $[Co^{II}(OH_2)_6](NO_3)_2$ (magenta line). The green line was obtained by subtraction of the appropriately weighted metal spectrum from the spectrum of the Co-N-C material after catalytic operation assuming that 28% of film consisted of purely metallic cobalt. The resulting spectrum was renormalized and Fourier-transformed. This spectrum (green line) is assignable to a non-metallic species with light atoms (O, N, C) in the first coordination sphere of cobalt (represented by $[Co^{II}(OH_2)_6]^{2+}$) and a cobalt-ligand distance of 2.1 Å. A more quantitative analysis is prevented by noise problems and the uncertainties in the used approach to correct for contributions of the metallic cobalt. The peaks in the EXAFS spectra are labeled with the corresponding Co-ligand distances.

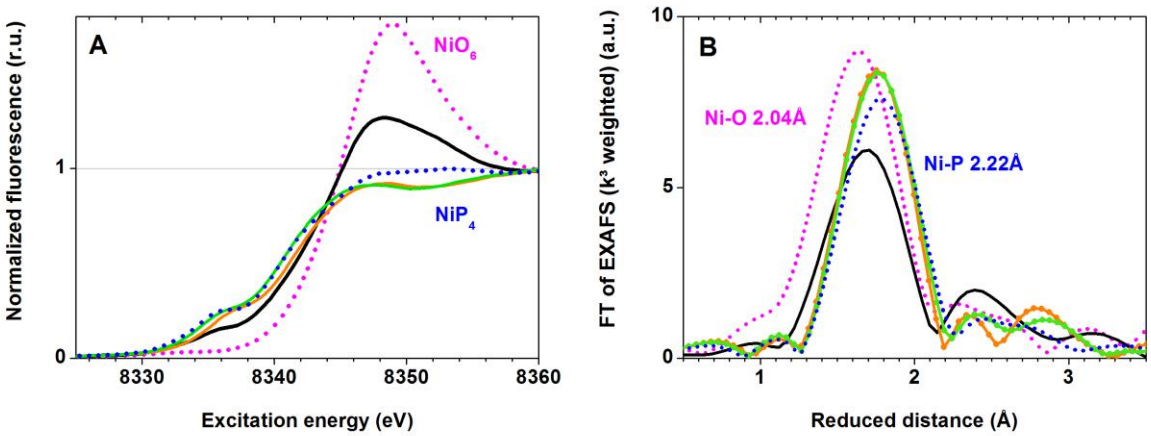

Figure S10: XANES spectra (A) and Fourier-transforms (*k*-range from 2 to 13 $Å^{-1}$) of k^3-weighted EXAFS spectra (B) at the Ni *K* edge. Black solid line: Ni-CNT as prepared. Orange solid line: Ni-CNT in direct contact with the electrolyte (aqueous 0.5M H_2SO_4) after equilibration with a few cyclic voltammograms. Green solid line: Ni-CNT in direct contact with the electrolyte (aqueous 0.5M H_2SO_4) after 1h of H_2 oxidation. Blue dotted line: pristine $[Ni(P^{Ph}{}_2N^{CH2pyrene}{}_2)_2]$. Magenta dotted line: $[Ni(OH_2)_6]^{2+}$. In B, the main peaks of $[Ni(P^{Ph}{}_2N^{CH2pyrene}{}_2)_2]$ and $[Ni(OH_2)_6]^{2+}$ are labelled with the corresponding Ni-ligand distance.

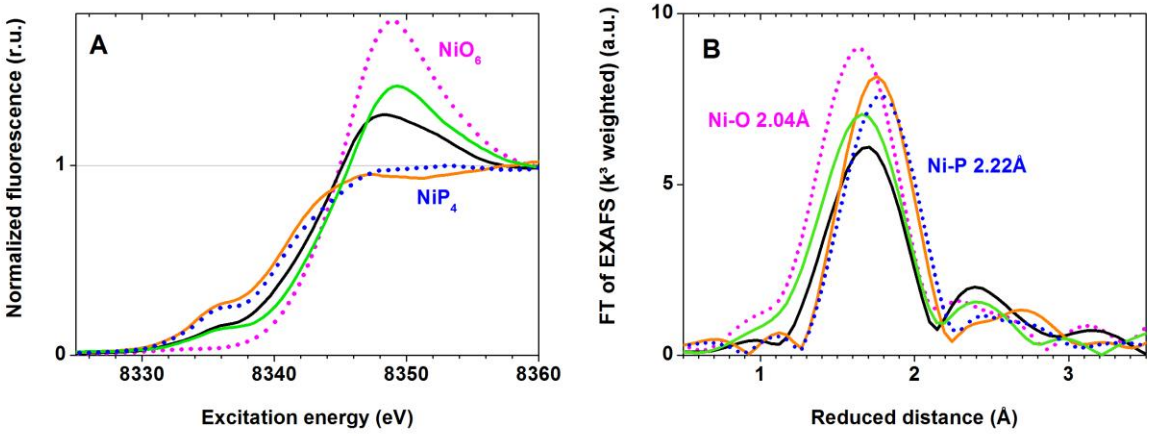

Figure S11: XANES spectra (A) and Fourier-transforms (*k*-range from 2 to 13 $Å^{-1}$) of k^3-weighted EXAFS spectra (B) at the Ni *K* edge. Black solid line: Ni-CNT as prepared. Green solid line: Ni-CNT coated onto a Nafion membrane after 1h of H_2 evolution. Orange solid line: Ni-CNT in direct contact with the electrolyte (aqueous 0.5M H_2SO_4) after 1h of H_2 evolution. Blue dotted line: pristine $[Ni(P^{Ph}{}_2N^{CH2pyrene}{}_2)_2]$. Magenta dotted line: $[Ni(OH_2)_6]^{2+}$. In B, the main peaks of $[Ni(P^{Ph}{}_2N^{CH2pyrene}{}_2)_2]$ and $[Ni(OH_2)_6]^{2+}$ are labelled with the corresponding Ni-ligand distance.

	Ni-ligand distance [Å]		Coordination number	
	Ni-O	Ni-P	Ni-O	Ni-P
$[Ni(OH_2)_6]^{2+}$	2.03		6	
$[Ni(P^{Ph}{}_2N^{CH2pyrene}{}_2)_2]$		2.22		4
Ni-CNT as prepared	2.04	2.23	2.0	1.9
Ni-CNT in direct contact with the electrolyte (aqueous 0.5M H_2SO_4)				
after electrochemical equilibration		2.18		3.5
after 1h H_2 oxidation		2.19		3.6
after 1h H_2 evolution		2.19		3.9
Ni-CNT coated with a Nafion membrane				
after 1h H_2 evolution	2.00	2.25	2.5	1.6
E_0=1.6 eV $S_0{}^2$=0.76	Ni-O $2\sigma^2$=0.009 Å^2 Ni-P $2\sigma^2$=0.004 Å^2			

Table S2. Overview of the Ni-P distances and coordination P numbers of the bio-inspired NiP_4 catalyst in its pristine state, grafted on CNT ("Ni-CNT"), after electrochemical equilibration, after H_2 oxidation and after H_2 evolution. It is differentiated between conditions where the Ni-CNT material was in direct contact with the electrolyte or coated with a Nafion membrane. If a Ni-O/N/C species is significantly present besides the NiP_4 catalyst, then its Ni-O distance and O coordination number is given. The Ni-P/O distances and coordination numbers were determined by fitting the corresponding EXAFS spectra with two phase-functions: one for P and one for O. The functions were calculated from crystal structures similar to $[Ni(P^{Ph}{}_2N^{CH2pyrene}{}_2)_2]$ or $[Ni(OH_2)_6]^{2+}$, respectively. For all fits, the energy offset, E_0, the amplitude reduction factor, S_0, and the Debye-Waller parameters, σ, of P and O were fixed at values determined from fits of the corresponding references, $[Ni(P^{Ph}{}_2N^{CH2pyrene}{}_2)_2]$ or $[Ni(OH_2)_6]^{2+}$. For E_0 and S_0, the averages of the yielded values from the reference fits were applied. The use of an average but suboptimal S_0 leads to erroneous coordination numbers due to a correlation between those two fit parameters. In this case, the coordination numbers of P are suppressed and the ones of O are amplified. For compensation, all coordination numbers were multiplied by specific scale factors for P and O. These factors were determined via fitting the references with the average values for E_0 and S_0 and dividing the correct coordination numbers for P (N=4) and O (N=6) by the yielded coordination numbers.

References:

1. P. D. Tran, A. Le Goff, J. Heidkamp, B. Jousselme, N. Guillet, S. Palacin, H. Dau, M. Fontecave and V. Artero, *Angew. Chem. Int. Ed.*, 2011, **50**, 1371-1374.
2. F. Schaefers, M. Mertin and M. Gorgoi, *Rev. Sci. Instrum.*, 2007, **78**.
3. M. Risch, K. Klingan, J. Heidkamp, D. Ehrenberg, P. Chernev, I. Zaharieva and H. Dau, *Chem. Commun.*, 2011, **47**, 11912-11914.
4. J. A. Bearden and A. F. Burr, *Reviews of Modern Physics*, 1967, **39**, 125-&.
5. A. J. Bard and L. R. Faulkner, Electrochemical Methods, Fundamentals and Applications, Wiley, New York, (2001).
6. Y. Gochi-Ponce, G. Alonso-Nunez and N. Alonso-Vante, *Electrochem. Commun.*, 2006, **8**, 1487-1491.
7. K. L. Hsueh, E. R. Gonzalez and S. Srinivasan, *Electrochim. Acta*, 1983, **28**, 691-697.
8. A. Morozan, P. Jegou, B. Jousselme and S. Palacin, *Phys. Chem. Chem. Phys.*, 2011, **13**, 21600-21607.
9. F. Jaouen, J. Herranz, M. Lefevre, J. P. Dodelet, U. I. Kramm, I. Herrmann, P. Bogdanoff, J. Maruyama, T. Nagaoka, A. Garsuch, J. R. Dahn, T. Olson, S. Pylypenko, P. Atanassov and E. A. Ustinov, *ACS Appl. Mater.Interf.*, 2009, **1**, 1623-1639.
10. S. L. Gojkovic, S. Gupta and R. F. Savinell, *J. Electrochem. Soc.*, 1998, **145**, 3493-3499.
11. J. R. Pels, F. Kapteijn, J. A. Moulijn, Q. Zhu and K. M. Thomas, *Carbon*, 1995, **33**, 1641-1653.
12. R. L. Arechederra, K. Artyushkova, P. Atanassov and S. D. Minteer, *ACS Appl. Mater. Interf.*, 2010, **2**, 3295-3302.
13. K. Artyushkova, S. Levendosky, P. Atanassov and J. Fulghum, *Top. Catal.*, 2007, **46**, 263-275.
14. T. S. Olson, S. Pylypenko, J. E. Fulghum and P. Atanassov, *J. Electrochem. Soc.*, 2010, **157**, B54-B63.
15. S. Kundu, T. C. Nagaiah, W. Xia, Y. M. Wang, S. Van Dommele, J. H. Bitter, M. Santa, G. Grundmeier, M. Bron, W. Schuhmann and M. Muhler, *J. Phys. Chem. C.*, 2009, **113**, 14302-14310.